Europe PMC Funders Group
Author Manuscript
J Immunol. Author manuscript; available in PMC 2017 November 15.

Published in final edited form as:
J Immunol. 2017 May 15; 198(10): 3999–4011. doi:10.4049/jimmunol.1601473.

Antibody distance from the cell membrane regulates antibody effector mechanisms

Kirstie L.S. Cleary, **H.T. Claude Chan**, **Sonja James**, **Martin J. Glennie**, and **Mark S. Cragg**
Antibody & Vaccine Group, Cancer Sciences Unit, Faculty of Medicine, University of Southampton, Southampton General Hospital, Southampton, SO16 6YD, UK

Abstract

Immunotherapy using monoclonal antibodies (mAb) such as rituximab is an established means of treating haematological malignancies. Antibodies can elicit a number of mechanisms to delete target cells, including complement dependent cytotoxicity (CDC), antibody dependent cellular cytotoxicity (ADCC) and antibody dependent cellular phagocytosis (ADCP). The inherent properties of the target molecule help define which of these mechanisms are more important for efficacy. However, why mAb binding to different epitopes within the same target elicits different levels of therapeutic activity, is often unclear.

To specifically address whether distance from the target cell membrane influences the aforementioned effector mechanisms, a panel of fusion proteins consisting of a CD20 or CD52 epitope attached to various CD137 scaffold molecules were generated. The CD137 scaffold was modified through the removal or addition of cysteine-rich extracellular domains, to produce a panel of chimeric molecules which held the target epitope at different distances along the protein.

It was shown that CDC and ADCC favoured a membrane proximal epitope, whilst ADCP favoured an epitope positioned further away. These findings were then confirmed using reagents targeting the membrane proximal or distal domains of CD137 itself before investigating these properties *in vivo* where a clear difference in the splenic clearance of transfected tumour cells was observed. Together, this work demonstrates how altering the position of the antibody epitope is able to change the effector mechanisms engaged and facilitates the selection of mAbs designed to delete target cells through specific effector mechanisms and provide more effective therapeutic agents.

Keywords

monoclonal antibody; immunotherapy; direct targeting; membrane distance; CDC; ADCC; ADCP; epitopes; complement; phagocytosis

Correspondence: Mark S. Cragg, University of Southampton, Southampton General Hospital, Southampton, SO16 6YD, UK (FAX: +44 (0) 23 80704061; msc@soton.ac.uk).

Abbreviations used: ADCC, antibody dependent cellular cytotoxicity; ADCP, antibody dependent cellular phagocytosis; BMDM, bone marrow derived macrophages; CDC, complement dependent cytotoxicity; RTX, rituximab; WGA, wheat germ agglutinin; WT, wild type

Conflict of Interest Disclosure

MSC is a retained consultant for Bioinvent and has performed educational and advisory roles for Baxalta. He has received research funding from Roche, Gilead and GSK. MJG is an advisor to BioInvent International.

Europe PMC Funders Author Manuscripts
Europe PMC Funders Author Manuscripts

Europe PMC Funders Author Manuscripts

Europe PMC Funders Author Manuscripts

Introduction

In the last decade monoclonal antibody (mAb) immunotherapy has become an established treatment for cancer. Initially in haematology, based upon the success of the anti-CD20 mAb rituximab (1), mAb are now becoming central to the treatment of many solid and difficult to treat cancers (2). mAb such as rituximab are referred to as direct targeting mAb and as such bind directly to the tumour cell target facilitating tumour clearance via Fc independent; (direct cell death (3, 4)); or Fc dependent mechanisms (complement dependent cytotoxicity (CDC), antibody dependent cellular phagocytosis (ADCP) and antibody dependent cellular cytotoxicity (ADCC)(5)). Understanding what facilitates or impairs these mechanisms is pivotal for the development of more effective therapeutics.

CDC involves the initiation of the Classical complement pathway following the interaction of C1q with at least 2 antibody Fc regions in close proximity (6), with hexameric conformation of antibody complexes demonstrated to be highly efficient (7). The proteolytic cascade continues resulting in inflammation via C3 or ultimately the insertion of the membrane attack complex into the target cell membrane and potential cell lysis. In addition soluble components, such as C3a and C5a, are produced which facilitate the recruitment of immune effector cells such as neutrophils and macrophages which interact with complement receptors to initiate activation and phagocytosis (8, 9). Both ADCC and ADCP are mediated via activatory Fcγ-receptors (FcγR) expressed on immune cells such as Natural Killer (NK) cells and myeloid cells (10). For ADCC, binding of the FcγR on NK cells culminates in the release of cytotoxic granules (containing perforin and granzymes) which enter the targeted cell resulting in cell death (11). In contrast, for ADCP, FcγR activation results in cytoskeletal rearrangements, allowing the formation of a phagosome (12). The mAb-coated cell is then endocytosed and degraded by lysosomal enzymes present within (13).

Which effector mechanism is most important for the efficacy of direct targeting mAbs in humans is widely debated. Pivotal work in 2000 demonstrated the therapeutic activity of anti-CD20 mAbs was dependent on the presence of activatory FcγR in mice, and was limited by the presence of the inhibitory FcγR IIB, CD32B (14). This dependence on FcγR is not restricted to anti-CD20 mAb as it has also been reported for anti-EGFR mAb directed at solid tumours (15). More recently, there is a growing body of work that proposes myeloid cells as the FcγR-expressing effectors and ADCP as the predominant effector mechanism for this class of mAb (16, 17).

Ever since the initial generation of mAbs it has been known that different mAb to the same target can elicit widely different activities (18); including differences in the effector mechanisms engaged. For example, type II anti-CD20 mAb do not elicit CDC efficiently whereas type I mAb do (19, 20) and ofatumumab is more efficient at CDC compared to rituximab (21). These mechanistic differences are not unique to anti-CD20 mAbs; trastuzumab is reported to better engage ADCC compared to pertuzumab (18). Importantly, these differences are not a simple consequence of the antibody isotype (22), therefore it is logical to conclude that the nature of the epitope bound influences the effector mechanism engaged.

Europe PMC Funders Author Manuscripts

Europe PMC Funders Author Manuscripts

As of July 2015 there were 22 mAbs approved or pending approval for the treatment of cancer in the US and EU (23). Nearly two thirds are direct targeting mAbs against only 8 different antigens. Many more targets have been assessed in oncology and so it is currently unclear what makes these targets so effective as antigens for mAb-mediated immunotherapy. Various explanations for the relationship between the antigen and mAb effector mechanisms have been proposed; relating to antigen density, size, position on the target and mobility. Antigen expression levels have been correlated to anti-CD20 mAb efficacy (21, 24) and work performed by Derer *et al* demonstrated that the engagement of CDC was more dependent on the expression level of EGFR compared to NK mediated ADCC (25). However, it has long been known that antigen specificity (and not simply antibody isotype or expression level) was an important factor in determining the efficacy of CDC (26). Another observation is that the targets approved for cancer immunotherapy are generally small proteins (18, 27), or if a larger protein (such as Her2) the antibody binds relatively close to the cell membrane (28). Accordingly, two of the most successful targets in oncology, and highly represented in the list of approved reagents, are CD20 and CD52 – both of which are highly-expressed surface receptors with small extracellular domains.

Targeting small antigens, or membrane proximal epitopes, has previously been shown to be beneficial for chimeric antigen receptor T cells; where a decrease in the T cell cytotoxicity was observed when binding domains were positioned further away from the target cell (22, 29). However, this property has not been directly investigated for mAb immunotherapy. We therefore hypothesised that the distance an epitope lies from the target cell membrane was important for mAb immunotherapy, particularly for the engagement of the Fc-mediated mechanisms CDC, ADCP and ADCC. To investigate this directly, avoiding the potential caveats arising from using mAb with different affinities and/or targeting subtly different mAb epitopes, we generated a panel of fusion proteins based upon a CD137 scaffold displaying exactly the same target epitope recognised by either rituximab or CAMPATH-1H at different distances from the target cell membrane. These proteins were then expressed in a variety of target cells and used as model antigens in deletion assays *in vitro* and *in vivo.* We found that the effector mechanisms engaged by both anti-CD20 and anti-CD52 mAb were dependent on the fusion protein targeted and its distance from the cell surface. This work has important implications for the development of new therapeutics which seek to exploit specific effector mechanisms and elicit more effective deletion.

Materials and Methods

Antibodies

F4/80-APC was from SeroTec (clone CI:A3-1); B220-PerCP (clone RA3-6B2), anti-mouse-Fc-Fab_2-PE (clone Poly4053), CD55-PE (clone RIKO-3) and CD59-PE (clone mCD59.3) were purchased from BioLegend. Rituximab-hIgG1 and rituximab-mIgG2a were produced in-house from patented sequences (22); CAMPATH-1H was kindly provided by Drs Steve Cobbold and Geoff Hale; A20 anti-Idiotype (clone 1G6 (30)) was provided by Professor Ron Levy; anti-human CD137 mAbs, SAP1-3 and SAP3-6, were produced in-house as part of the Southampton Antibody Discovery Programme (CRUK). Polyclonal anti-human CD137 (clone ab197942) antibody used for western blotting was from Abcam.

Europe PMC Funders Author Manuscripts

Europe PMC Funders Author Manuscripts

Cell Culture

Bone marrow derived macrophages (BMDM) were generated from the bone marrow of wild type BALB/c female mice collected and cultured at $0.8x10^6$ cell/mL in 6 well plates for 8 days in RPMI media supplemented with 10% Foetal Calf Serum (FCS), 2mM glutamine, 1mM sodium pyruvate, and 20% L929 conditioned media (containing GM-CSF) at 37°C in 5% CO_2. CHO-S cells were from Invitrogen, and cultured in serum free FreeStyle CHO media, in a shaking incubator at 37°C in 5% CO_2. A20 cells (31) were cultured in RPMI media supplemented with 10% FCS, 2mM glutamine, 1mM pyruvate, 100 IU/mL penicillin and streptomycin (all from Gibco) at 37°C in 5% CO_2.

Cloning of fusion constructs

Fusion constructs were cloned through overlap extension PCR (32) using wild type human CD137 (UniProt: Q07011; NCBI ref: NM_001561), human CD52 (Uniprot: P31358; NCBI ref: NM_001803.2) or the Rp3/Cp11 epitope (kind gift of Prof Martin Pule and Dr Brian Philip, UCL (33, 34)). Each fusion protein consisted of the CD52 leader sequence, Rp3/Cp11, CD137 (with domains removed based on the annotations provided with Uniprot reference sequence). These gene constructs were cloned into pcDNA3.1/- (neo) expression vector (Invitrogen).

Cell Transfections

$10x10^6$ CHO-S cells were transfected with 10μg of plasmid DNA using lipofection with FreeStyleMax (Invitrogen). A20 cells were nucleofected using Kit T from Lonza with 2μg of plasmid DNA. Following nucleofection, cells were cultured in the presence of 1mg/mL geneticin (Gibco) to select for stable transfectants.

CDC assay

$1x10^5$ cells were labelled with diluting concentrations of antibody for 15 minutes at room temperature. Human serum (Sigma) was added at 15% final concentration (v/v) and incubated at 37°C for 30 minutes. Cell death was assessed with propidium iodide inclusion by flow cytometry using a FACScan (BD). Non-opsonised cells were used to establish basal cell death and the raw data adjusted to the transfection efficiency using the following equation:

CDC-specific lysis = [(%PI^+ of sample − baseline / 100 − %PI^+ baseline)*100]/%transfected cells * 100

ADCP assay

Target cells were labelled with 5μM CFSE for 10 minutes at room temperature before washing in complete media. CFSE labelled targets were then opsonised with diluting concentrations of antibody before co-culturing at 5:1 Target (T): Effector (E) ratio with BMDM in 96 well plates for 1 hour at 37°C. BMDM were then labelled with anti-F4/80-APC for 15 minutes at room temperature and washed with PBS twice. Plates were kept on ice and wells scraped to collect BMDMs and phagocytosis assessed by flow cytometry using

Europe PMC Funders Author Manuscripts

a FACSCalibur (BD) to determine the percentage of F4/80+CFSE+ cells within the F4/80+ cell population.

Confocal imaging of ADCP

BMDMs were plated overnight at $1x10^5$ cells/mL onto poly-L-lysine (Sigma) coated coverslips. Target cells were labelled with CFSE and 10μg/mL of antibody as described above in "ADCP assay". Following the 1 hour co culture, coverslips were washed in PBS before fixation in 2% paraformaldehyde for 15 minutes at room temperature. 100μg/mL of Rhodamine Wheat Germ Agglutinin (WGA) was added for 30 minutes at room temperature before washing in PBS. Lastly nuclei were stained with DAPI before mounting. Images were collected on a Leica TCS SP5 (Leica Microsystems) using Leica software (LAS-AF v2) and processed using Adobe Photoshop CC (version 7 SP1).

ADCC assay

Target cells were labelled with calcein-AM, followed by the addition of diluting concentrations of antibody. Target cells were then co-cultured with human PBMC at a 50:1 E:T ratio for 4 hours at 37°C. The plate was then centrifuged at 400g for 5 minutes to pellet the cells and the supernatant transferred to a white 96-well plate. Calcein release was measured using a VarioSkan (ThermoScientific) at 455nm, and the percentage of maximal release calculated as follows:

% max release = (sample / TX-100)*100

In vivo experiments

All animal experiments were performed in accordance with the Animal (Scientific Procedures) Act 1986 within a Home Office approved facility under project licence 30/2964. Wild type (WT) female BALB/c mice under 4 months of age were used, and all procedures determined as mild until the experimental end point. $1x10^6$ A20 cells were administered intravenously on day 0. On day 3, 100μg of rituximab-mIgG2a (22) or PBS was given by i.v. injection. The spleen, liver and inguinal lymph nodes were collected from all mice when the control group developed terminal tumour burden (defined as visible signs of ill-health, including expansion of the liver). Organs were homogenised into a single cell suspension in 3mL of sterile PBS, and passed through a 100μm cell strainer before analysis by flow cytometry.

Western Blotting of cell lysates

$6x10^6$ cells were lysed in RIPA buffer (25mM Tris-HCL, 150mM NaCl, 1% NP-40, 1% sodium deoxycholate, 0.1% SDS, containing protease inhibitor cocktail (Sigma), 50mM NaF and 0.2mM Na_3VO_4). 25μg of lysate was loaded onto 10% Bis-Tris gels, and proteins separated under constant voltage. The proteins were transferred onto a nitrocellulose membrane, blocked using a 5% milk solution (Marvel) and probed with a polyclonal rabbit anti-human CD137 antibody overnight at 4°C. The membrane was washed, and bound antibody detected using a HRP-conjugated anti-Rabbit secondary (GE Healthcare, NA9340) and ECL substrate (ThermoScientific) before chemiluminesence film was applied and developed using a Xograph Imaging Systems Compact X4.

Europe PMC Funders Author Manuscripts

Europe PMC Funders Author Manuscripts

Statistics

Data were analysed using a one or two-way ANOVA where appropriate. All statistical analyses were performed in GraphPad Prism (version 7.01).

Results

Generation of a model antigen system

A panel of engineered molecules were designed to assess the relationship between the epitope targeted along a target protein (from its membrane proximal to distal domains) and the effector mechanisms engaged. These first constructs contained a small peptide (previously identified to be bound by the anti-CD20 mAb rituximab (34)) attached to the N-terminal domain of human CD137. Human CD137 contains four fairly equivalently sized extracellular cysteine-rich domains (Figure 1A) and so is ideal for modular manipulation (35). Through the use of overlap extension PCR, extracellular domains were removed or replicated resulting in a panel of fusion proteins designed to display the rituximab epitope at varying distances from the cell surface estimated to range from 0.3 - 16 nm away (Figure 1A). These constructs were transiently transfected into CHO-S cells, with protein expression confirmed by flow cytometry using antibodies directed against the rituximab epitope and individual domains of CD137 (Figure 1B and manuscript in preparation). Importantly the position of the epitope did not appear to change binding and rituximab bound equally well at all positions along CD137. Western blotting was also performed in particular to confirm the size difference between the R-4d and R-8d constructs (not possible by flow cytometry due to the duplication of the same extracellular domains in CD137; Figure 1C).

Assessment of antibody effector engagement with rituximab

CHO-S cells expressing each of the fusion proteins were used as targets in order to assess whether the ability of rituximab to engage CDC, ADCP or ADCC was altered dependent on the distance the epitope was held from the cell membrane. The first mechanism investigated was CDC, where cells were cultured with rituximab (RTX) in the presence of human serum, and cell death recorded by flow cytometry (Figure 2A). In preliminary experiments, using CHO-S cells expressing the R-4d construct as targets, a serum titration was performed where it was found that maximal killing could be achieved at 15% serum, with no further improvement even when the serum concentration was increased to 45% (Supplemental Figure 1). As such, 15% serum was used in all subsequent CDC assays. To adjust for any differences in protein expression of the different constructs, the degree of target cell lysis was corrected according to the level of expression as described in the methods. These experiments showed clearly that the ability of RTX to initiate CDC was diminished when targeted furthest away from the cell surface with the R-8d construct (Figure 2B). Less than half of the cells were lysed under saturating (10μg/mL) concentrations of antibody, with little-to-no lysis observed when the antibody concentration was ≤ 0.4μg/mL. Although the other three constructs were able to engage CDC similarly at the higher mAb concentrations, R-4d showed a trend (although not statistically significant) towards being less effective as a target at lower concentrations of antibody (< 0.4μg/mL) compared to constructs targeting the mAb closer to the cell surface (R-1d and R-flush).

Europe PMC Funders Author Manuscripts

Europe PMC Funders Author Manuscripts

Next, we assessed the ability of the constructs to function as targets for phagocytosis using mouse bone marrow derived macrophages (BMDM) as effectors (Figure 2C). In these ADCP assays targeting all of the constructs except for R-flush resulted in effective phagocytosis of RTX-opsonised targets (Figure 2D). Although at lower concentrations of antibody (< 1μg/mL) R-8d was less sensitive to ADCP compared to the R-1d and R-4d, this was not statistically significant. Importantly, expression of the R-flush domain was equivalent to the other constructs (Figure 1B), and sufficient for effective CDC (Figure 2B), indicating that displaying the antigen too close to the cell surface was specifically detrimental to phagocytosis as opposed to simply being inaccessible to mAb binding.

The ability of the various constructs to mediate ADCC activity was also evaluated. Human PBMCs were used as the source of effector cells in these assays, with the resident NK cells previously shown to be the main mediators of cytotoxic activity (36). Targeting R-flush resulted in the best engagement of ADCC, whilst targeting R-8d elicited the lowest level of killing (Figure 2E), similar to the trend seen with CDC.

Assessment of antibody effector engagement with CAMPATH-1H

To confirm that the results generated above were related to antibody distance and not a unique property of the RTX epitope, a second panel of fusion proteins were generated. These contained the same CD137 backbone as before (Figure 1A); but with the RTX epitope replaced for one recognised by the anti-CD52 antibody, CAMPATH-1H (alemtuzumab) (33). These proteins were expressed in CHO-S cells and recognised specifically by CAMPATH-1H (Figure 3A) and not RTX (data not shown). When used as targets in the three *in vitro* assays (Figure 3B-C) the same trends in terms of distance and the effector mechanism engaged were identified such that CDC and ADCC were ineffective when targeted furthest away from the target cell membrane (C-8d) and ADCP was sub-optimal when targeted too close to the cell membrane (C-flush).

Stable expression compared to transient expression systems

The engagement of antibody effector mechanisms, such as CDC, can be influenced by the expression levels of the targeted antigen (21, 24, 25). The transient transfection approach presented previously resulted in a heterogeneous population containing both non-transfected cells and cells with a range of expression levels for each fusion protein, including a proportion of cells expressing extremely high levels of target (Figure 1B and Figure 3A). Whilst this approach is useful for avoiding potential selection artefacts, it may obscure more subtle observations at lower expression levels occurring as a consequence of distance. In order to determine whether the engagement of the FcγR-dependent effector mechanisms were affected by the antigen expression level, the murine cell line A20 was transfected with R-4d and stable clones of different expression levels were isolated (Figure 4A). These clones (referred to as R-4d-Low, R-4d-Med and R-4d-High) were assessed in the FcγR mediated assays, ADCP (Figure 4B) and ADCC (Figure 4C). In both cases, there was a clear decrease in the ability to engage these mechanisms when targeting antigen expressed at lower levels, although the difference between the high and medium expressing clones are not statistically significant.

Europe PMC Funders Author Manuscripts

Europe PMC Funders Author Manuscripts

Having established this clear relationship, to exclude this variable when comparing between the panel of proteins, the A20 cell line was transfected with the rituximab binding fusion constructs (R-flush, R-4d and R-8d) to produce a panel of stable cell lines with equivalent expression levels (Figure 5A). These cells were used as targets in the three effector assays. As seen in Figure 5B-D, the results confirmed the observations reported for the transient CHO-S system i.e. CDC and ADCC were diminished when targeting the cells displaying the R-8d construct and ADCP was poor when targeting the R-flush transfected cells. These data provide further evidence that the effector mechanisms engaged by an antibody are directly influenced by the epitope distance from the target cell membrane.

Having established these principles in a controlled system we then sought to validate them using a more typical scenario where antibodies are available to different epitopes on the same target molecule. This approach also has the added advantage that the expression profile of the target molecule, and the target cell itself is exactly the same for both of the mAbs used. Utilising a recently generated pair of anti-CD137 mAb with similar affinities (manuscript in preparation), known to bind the most proximal (SAP3-6) or distal (SAP1-3) domains of CD137 (Figure 1A) we explored their relative efficacy in CDC, ADCP and ADCC. In both the CDC and ADCC assays, the most membrane proximal mAb, SAP3-6, was more effective than the distal mAb (Figure 6A and 6C), particularly in ADCC. In contrast, in our ADCP assay (Figure 6B), there was no clear difference between the two antibodies, both being able to elicit significant phagocytosis compared to the isotype control. The similarity observed between SAP1-3 and SAP3-6 in the ADCP assay was comparable to that reported earlier between the 4-domain and 1-domain constructs (Figures 2D and 3C). This indicates that whilst SAP3-6 binds the bottom domain of CD137, it is at a similar distance from the cell membrane as the R-1d construct (rather than R-flush), and so is ideal for ADCP. This data further corroborates the distance hypothesis that binding close to the target cell membrane is preferable for ADCC and CDC.

Resolving the conflict between Cp11-flush and WT-CD52 in ADCP assay

The work presented thus far demonstrated that engagement of the mAb effector mechanisms were influenced by the distance an antibody binds from the target cell membrane, initially with RTX and subsequently with CAMPATH-1H. Human CD52, the antigen for CAMPATH-1H, consists of a 12 amino acid extracellular peptide tethered to the cell membrane via a glycophosphatidylinositol (GPI) anchor (37, 38). This is similar to the C-flush construct generated within this study, which contained an 11 amino-acid extracellular peptide tethered via a protein transmembrane domain (Figure 1A). *In vitro* CAMPATH-1H is highly effective at engaging CDC to delete target cells(39) whilst *in vivo,* human and murine studies indicate that the effectiveness and prolonged clearance observed are primarily FcγR meditated (40, 41). Given the key role of macrophages for antibody immunotherapy (17, 42), it is therefore logical to assume that CAMPATH-1H is also effective in ADCP. However, in Figure 3C, we demonstrated that CAMPATH-1H was unable to effectively elicit phagocytosis when targeting the C-flush construct. Knowing that the engagement of CDC and ADCC by CAMPATH-1H when binding the C-flush construct fitted the expected mechanism of action for this mAb (Figures 3B and 3D), the poor phagocytosis when binding an antigen similar to its natural target warranted further

Europe PMC Funders Author Manuscripts

Europe PMC Funders Author Manuscripts

investigation. This was not the consequence of the CHO-S transient expression system used, since transfecting these cells with WT CD52, followed by CAMPATH-1H resulted in highly effective ADCP (Supplemental Figure 2A), indicating that the C-flush construct must differ in some other key property.

Both proteins consist of small extracellular domains, however CD52 is glycosylated just outside of the CAMPATH-1H epitope whereas the C-flush construct is not (37, 43). It was therefore postulated that the presence of the glycan on CD52 may stabilise the interaction of CAMPATH-1H leading to preferential ADCP compared to the C-flush fusion protein. A mutant form of CD52 (referred to as CD52-NQ), where the Asn was mutated to a Gln, was generated, expressed on CHO-S cells (Supplemental Figure 2B) and assessed in the ADCP assay (Figure 7A). The non-glycosylated mutant was still able to elicit ADCP following CAMPATH-1H treatment demonstrating that glycosylation of CD52 was not important for the effective induction of ADCP by CAMPATH-1H.

We next considered whether the method of membrane attachment was influencing the efficiency of ADCP. To test this a GPI-anchored version of the CAMPATH-1H epitope was generated. The C-GPI construct contained the same leader and carboxy-terminal sequences as human CD52, as well as the Pro-Ser of the CD52 GPI attachment site (Figure 7B). This was based on previous work which proposed that two amino-acids prior to the GPI attachment site and the carboxy-sequence were important for mediating the post-translational attachment of the protein to the GPI anchor (44, 45). The C-GPI construct was expressed in CHO-S cells (Supplemental Figure 2C), bound by CAMPATH-1H, and then compared in ADCP assays alongside C-flush and WT CD52 (Figure 7C). These experiments clearly demonstrated a rescue in ADCP function when the CAMPATH-1H epitope was tethered through the GPI format (C-GPI), leading to a construct that was at least as efficient as WT CD52 and far more effective than C-flush. These data indicate that the GPI anchor likely overcomes the restriction on ADCP for targets that are extremely close to the cell surface.

In vivo function of rituximab targeting different distances

Investigating the effector mechanisms in individual effector assays *in vitro* clearly identified differences between the most proximal and distal epitope constructs, R-flush and R-8d, respectively. To explore the relevance of these findings for immunotherapy *in vivo* where all mechanisms might be in play we used the A20 cells, stably transfected with either R-flush or R-8d (Figure 5A). These were injected intravenously (i.v.) into WT female BALB/c mice and the resulting tumours were detected and distinguished from endogenous B cells using flow cytometry with an A20 specific anti-idiotype mAb (Figure 8A). At terminal tumour burden, the A20 cells were located predominantly in the spleen and liver.

To compare the capacity of these two different antigens to facilitate tumour deletion, three days following tumour inoculation a single dose of PBS or RTX-mIgG2a was administered (Figure 8B) and the presence of A20 cells expressing each construct was determined in the spleen and liver. Although all groups had high tumour burden in the liver, leading to them becoming terminal, when comparing the percentage of tumour cells present in the spleens, mice which received tumour cells expressing R-flush followed by RTX-mIgG2a were

effectively cleared compared to those receiving PBS (Figure 8C). In contrast, the tumours expressing the R-8d construct were not cleared in either location, indicating inefficient targeting of the relevant effector mechanisms.

Discussion

Although mAb are increasingly used in the clinic to treat an ever expanding array of diseases there is still much that we do not know about this class of therapeutics. The diversity of molecules targeted by mAb has exponentially increased over the last decade (23) but surprisingly we are still ignorant of some of the most basic rules for their behaviour. Perhaps the simplest class of therapeutic mAb to understand are the direct targeting mAb. These reagents bind directly to the tumour cell target and elicit anti-cancer effects either by inducing changes to signalling (direct cell death) or by engaging Fc-mediated effector functions such as CDC, ADCP and ADCC. Although it is accepted that different mAb binding to the same target can elicit striking differences in therapeutic efficacy, evidence for why this may be is often scarce.

mAb properties such as FcγR affinity (46), isotype (47) and binding level (24, 25) have well-established effects on mAb effector systems and can certainly help explain why some mAb are more active than others. However, for other mAb, more subtle differences can also have a major impact. For example, in the case of the anti-CD20 mAb, type I and II engage different effector functions (4, 22) whilst binding to an overlapping, cross-blocking epitope (48). Given that several successful and approved anti-tumour mAbs bind to surface proximal antigens such as CD20 and CD52, here, we examined the effect that the position along a target molecule from membrane proximal to distal had on the effector mechanisms engaged by direct targeting antibodies.

The target molecule chosen, CD137, has four extracellular cysteine-rich domains (35). To date its atomic structure has not been resolved but modelled upon the TNFR1 crystal structure (49), the four domains would appear to gravitate away from the plasma membrane in a relatively linear fashion (Figure 1A) and so it is likely that the positions along CD137 correspond to increasing distances from the target cell surface. However, it is important to note that some of our findings may have been influenced by our choice of receptor. For example, our previous data highlighted the particular potency of CD20 as a target molecule due to its ability to cluster and redistribute into lipid raft areas of the plasma membrane (19). CD137 is an integral membrane protein expressed on T cells, and is a member of the tumour necrosis factor receptor superfamily (50), forming trimers with its ligand for activation (51). Cross-linking of CD137 was subsequently shown to cause its redistribution to lipid raft regions at the contact site with ligand-expressing cells (52) and so like CD20 and CD52, CD137 may reflect a particularly potent target molecule which can become redistributed and concentrated within the plasma membrane to augment mAb effector mechanisms.

Using a combination of approaches involving transient and stable expression systems, both *in vitro* and *in vivo*, we were able to reveal differences in the ability to engage the three Fc mediated effector mechanisms dependent upon the position of the mAb epitope from the cell surface. For two different specificities (anti-CD20 and anti-CD52) CDC was ineffective

Europe PMC Funders Author Manuscripts
Europe PMC Funders Author Manuscripts

Europe PMC Funders Author Manuscripts

Europe PMC Funders Author Manuscripts

when targeting the epitope furthest away (R-8d, C-8d) from the membrane and was less sensitive at lower mAb concentrations when binding cells expressing the 4-domain constructs (R-4d and C-4d; Figures 2B and 3B). A similar trend was observed for ADCC (Figures 2E and 3D). ADCP displayed different requirements, where a minimum distance of a single extracellular domain was required before phagocytosis of the target cell was achieved and membrane distal epitopes (R-8d and C-8d) were still relatively effective as targets (Figures 2D and 3C). Importantly, the ineffective phagocytosis of the membrane-flush epitopes (R-flush and C-flush), was not due to an inability of the antibody to bind these targets, as demonstrated by flow cytometry (Figures 1B and 3A) and their efficacy in the other effector assays (ADCC and CDC).

The effect of membrane distance on CDC is intuitively logical. The classical pathway of complement is known to be self-regulated by the short half-life of the active components at all stages of the cascade (53). Being activated far away from the target cell membrane has a reduced chance of stabilising on the cell surface due to the extended diffusion through the extracellular matrix. Therefore the greater the distance from the cell surface the lower the efficiency in the establishment of the C3 convertase complex – a key determinant in the cascade which leads to cell lysis via the formation of the membrane attack complex. This same reasoning was used to explain ofatumumab's superior engagement of CDC compared to rituximab; that it binds a more membrane proximal loop of human CD20 (5, 21).

More recent work has demonstrated that the activation of the classical complement pathway is better facilitated through a hexameric association of antibody Fc regions. Whilst the formation of hexamers can be engineered via Fc modification (54), they can form naturally upon the surface of the target cell via lateral movement of the antigen:antibody complexes (7). All of the constructs generated in this study contained identical transmembrane and intracellular domains – therefore it was assumed that they would have equivalent ability to redistribute across the cell surface and form hexamers. However, the extracellular domains of each construct vary in size. Differing levels of steric hindrance and interactions with other endogenous cell surface proteins could therefore influence membrane redistribution and restrict the hexameric complexes from forming.

All of the work presented within this study has used the human IgG1 isotype (or mouse IgG2a *in vivo* as the closest mouse parallel (10)), as this reflects the isotype typically adopted for direct targeting mAbs in the clinic (23). Whether other isotypes will follow the same rules remains to be determined as it is well established that they differ in their ability to engage the various effector mechanisms. Recently, hIgG3 has been investigated as an alternative to hIgG1 due to its superior engagement of FcγR (55) and binding of C1q (47) compared to hIgG1. Bruggemann *et al.* used a panel of chimeric antibodies containing the same specificity but class switched heavy chains to demonstrate that hIgG1 and hIgG3 were best at engaging CDC and ADCC (47). One interesting point is that although hIgG3 is better at binding C1q, this binding does not translate directly to improved CDC (26, 47). Other work reported that a chimeric antibody – containing the CH1 and hinge region of hIgG1 attached to a hIgG3 Fc domain – was better able at engaging CDC compared to WT-hIgG3 (56). One main difference between the hIgG1 and hIgG3 classes is the length of the hinge region, with hIgG3 having a hinge region approximately four times the size of hIgG1 (55).

Europe PMC Funders Author Manuscripts

Europe PMC Funders Author Manuscripts

In light of our work presented here, the improved lytic ability of the hIgG1/3 hybrid may be due to the far shorter hinge region, in turn bringing the complement activation closer to the cell surface for the engagement of CDC. It would be interesting to see whether combining this isotype chimera with epitopes directed to the membrane-proximal region of antigens would result in even more potent reagents.

Perhaps more surprising was the contrasting dependence on distance seen with the FcγR-mediated mechanisms, ADCP and ADCC. ADCP was significantly reduced when binding the membrane-flush constructs compared to those that were held at least one extracellular domain away (Figures 2D and 3C). ADCC was effective for these constructs but activity was lost when targeting an epitope positioned distal to the target cell membrane (Figures 2E and 3D). The approach undertaken within this study utilised the same epitope and mAb pairing, and as such the binding affinities remained consistent between all of the constructs investigated. In addition, the same antibody was used with no changes to the isotype or Fc region, therefore the kinetics behind the Fc:FcγR interactions would also be equivalent between systems. These observations reveal a fundamental difference between the requirements of activation for these mechanisms. Whilst both ADCC and ADCP require the engagement of activatory FcγR on the cell surface, the downstream effects and outcomes are clearly very different, although why this is the case currently remains unanswered.

Release of the cytotoxic granules by NK cells following FcγR activation has been demonstrated to utilise relatively small immune synapses, analogous to those induced during T cell mediated cytotoxicity (11). There is evidence that a T cell synapse needs to be less than 14nm in size in order to exclude any inhibitory signalling elements (such as the phosphatase CD45) from preventing activation, according to the kinetic-segregation model (57, 58). Assuming that the requirement for NK cell killing is similar, the fact that there is poor activation of ADCC when targeting the epitope held furthest away would fit this model, as the 8-domain fusion protein exceeds the maximum synapse size by approximately 2nm (58).

For phagocytosis, be it FcγR-mediated or via other means, there is a high level of intracellular reorganisation required in order to both form the phagosome and provide the means to engulf the targeted cell (12). This process is likely to last longer/require more continuous signalling compared to that for cytotoxic release; therefore the multimeric complex between the Ag, mAb and FcγR would need to be more stable and to mediate the sustained signalling required. Therefore, it is likely that when targeting the membrane-flush constructs, although the binding kinetics remain similar to that of the more distant epitopes, the endogenous proteins present within the cell membrane (not including the fusion protein itself) may provide steric resistance and pressures on the binding, resulting in an overall less stable multimeric complex; leading to less efficient ADCP. Phagocytosis is proposed to proceed through a zippering mechanism where integrins promote the efficient binding of FcγR:Fc complexes and serve to integrate signals from multiple, potentially disparate receptors (12). As zippering requires the formation of sequential FcγR:Fc complexes for continuing phagocytic cup generation and closure it could be that within this process, engagement of surface-proximal “flush” constructs do not facilitate appropriate integrin distribution or efficient zippering for the reasons listed above.

Europe PMC Funders Author Manuscripts

Europe PMC Funders Author Manuscripts

Antigen density has long been correlated with the effectiveness of CDC engagement both *in vitro* and in clinical studies (21, 24). High expression levels allow for a better chance of juxtaposed antibody Fc regions being present in the correct orientation for favourable engagement of C1 (6, 26). However the relationship between antigen expression level and the engagement of the FcγR-mediated mechanisms are less defined. Derer *et al.* indicated that NK and polymorphonuclear leukocyte mediated killing was less dependent on antigen expression compared to CDC, however there seemed to be a minimum level required before cell death was observed (25). It is worth noting that in that study different clones of antibody were used, potentially directed to different epitopes and with different affinities, rather than a single epitope and antibody targeted here, making it difficult to directly compare the efficacy of each epitope location. Nonetheless, using a range of cell-lines stably expressing different levels of the R-4d fusion protein it was clear that the percentage of ADCP and ADCC that occurred in response to RTX treatment positively correlated with the expression level (Figure 4). This finding agrees with the conclusions made by *Derer et al* in relation to CDC and ADCC (25) and supports other work from our group where the antigen expression level correlates positively with the amount of ADCP observed (manuscript in preparation).

Our further study of membrane proximal targets revealed an initial contradiction when targeting the native CD52, as opposed to the C-flush construct. We identified that attaching the CAMPATH-1H epitope mimic to a GPI anchor (C-GPI construct) restored sensitivity of the target cell towards phagocytosis (Figure 7C). GPI anchors are a commonly found post-translational modification, however there are still unknowns in terms of their structure, size and function. Resolved structures of GPI-anchors are lacking, however computer modelling indicate they may be far larger than anticipated, being around 1.5nm in size (59). Assuming CD52 utilises a similar anchor as modelled for CD59 (27, 59), then it is more equivalent in distance from the membrane to the C-1d construct, which is able to engage efficient ADCP, than the C-flush molecule, in support of our original hypothesis.

In vivo experiments in syngeneic immune competent mice revealed a clear depletion of A20 tumour cells expressing the R-flush but not R-8d construct from the spleen of BALB/c mice following treatment with RTX-m2a (Figure 8C). This indicates that the smaller, more membrane proximal epitope was more effective in depleting tumour cells and that ADCC and/or CDC were principally responsible. Although at odds with our recent findings indicating ADCP as the main effector mechanism (17, 60), it is reminiscent of our data with xenograft models (20) and likely reflects the use of a highly selected *in vitro* cell-line which has undergone loss of complement defence and/or NK control. The lack of complement defence through CD55 and CD59 was subsequently confirmed (Supplemental Figure 3). In contrast, no depletion was observed in the liver for either of the two tumour cell lines generated.

The differences in the clearance of R-flush expressing cells between the spleen and the liver reflect another factor that is yet to be clearly understood, the role of the tumour microenvironment in regulating mAb efficacy. It is now evident that the tumour microenvironment can promote infiltrating immune cells to adopt a more pro-tumour/immune-suppressive phenotype (61), however its direct effect on mAb therapy once again is unclear. Potentially, altering the epitope targeted within an antigen may allow for more

Europe PMC Funders Author Manuscripts

Europe PMC Funders Author Manuscripts

efficacious antibody therapies to be developed which can overcome the specific suppressive elements present. As well as direct anti-tumour targets this may also benefit reagents seeking to deplete immune-suppressive cells themselves – for example, regulatory T cells (T_{reg}) (62). Indeed the two anti-CD137 mAbs used here (SAP1-3 and SAP3-6) demonstrated an application of our findings (Figure 6). CD137 is expressed on resting T_{reg} and is upregulated following activation (63, 64) and so may serve as a useful target for T_{reg} deletion. Both SAP1-3 and SAP3-6 have the same isotype, bind to equivalent levels and with similar affinities towards CD137 (manuscript in preparation). Although they were broadly equivalent in their induction of ADCP, differences in the engagement of the effector mechanisms ADCC and CDC were apparent – particularly in relation to the minimum concentration required to elicit cell death. As both mAbs are in all other measurable ways equivalent, the difference likely lies in the bound epitope and its relation to the target cell membrane.

As detailed above, the tumour can manipulate its local microenvironment and has the capacity to impair the various effector mechanisms to circumvent mAb mediated killing. For example a highly suppressive macrophage environment might exist with a low activatory:inhibitory FcγR ratio but where complement components are plentiful. Similarly, if the environment is driving high levels of the FcγRIIB, NK-mediated ADCC may remain functional, as they, unlike macrophages, monocytes and dendritic cells do not express this inhibitory receptor. Using the knowledge gained here and switching the fine specificity of an antibody (i.e. the distance it binds from the cell surface), the most effective effector mechanisms can be selected in each situation; potentially leading to more potent antibody therapeutics.

Supplementary Material

Refer to Web version on PubMed Central for supplementary material.

Acknowledgements

The authors would like to thank all of the members of the Antibody and Vaccine Group for the discussions relating to the experiments reported herein and the Biomedical imaging unit for assistance with confocal microscopy. The Rp3/Cp11 epitope construct was a kind gift of Professor Martin Pule and Dr Brian Philip, UCL. The anti-idiotype for A20 was a kind gift of Professor Ron Levy. CAMPATH-1H was a kind gift of Drs Steve Cobbold and Geoff Hale. The domain-coloured image of TNFR1 structure was produced by Emma Sutton, using the 1TNR data file submitted within the Protein Data Bank.

Grant Support: Funding was provided through studentships from the BBSRC to KLSC and Programme Grants from Bloodwise (12050) and Cancer Research UK (A20537).

References

1. Molina A. A decade of rituximab: improving survival outcomes in non-Hodgkin's lymphoma. Annual review of medicine. 2008; 59:237–250.
2. Weiner LM, Murray JC, Shuptrine CW. Antibody-based immunotherapy of cancer. Cell. 2012; 148:1081–1084. [PubMed: 22424219]
3. Ivanov A, Beers SA, Walshe CA, Honeychurch J, Alduaij W, Cox KL, Potter KN, Murray S, Chan CH, Klymenko T, Erenpreisa J, et al. Monoclonal antibodies directed to CD20 and HLA-DR can elicit homotypic adhesion followed by lysosome-mediated cell death in human lymphoma and leukemia cells. The Journal of clinical investigation. 2009; 119:2143–2159. [PubMed: 19620786]

Europe PMC Funders Author Manuscripts

Europe PMC Funders Author Manuscripts

4. Alduaij W, Ivanov A, Honeychurch J, Cheadle EJ, Potluri S, Lim SH, Shimada K, Chan CH, Tutt A, Beers SA, Glennie MJ, et al. Novel type II anti-CD20 monoclonal antibody (GA101) evokes homotypic adhesion and actin-dependent, lysosome-mediated cell death in B-cell malignancies. Blood. 2011; 117:4519–4529. [PubMed: 21378274]
5. Oldham RJ, Cleary KLS, Cragg MS. CD20 and Its Antibodies: Past, Present, and Future. Forum on Immunopathological Diseases and Therapeutics. 2014; 5:7–23.
6. Borsos T, Rapp HJ. Complement fixation on cell surfaces by 19S and 7S antibodies. Science. 1965; 150:505–506. [PubMed: 5319759]
7. Diebolder CA, Beurskens FJ, de Jong RN, Koning RI, Strumane K, Lindorfer MA, Voorhorst M, Ugurlar D, Rosati S, Heck AJ, van de Winkel JG, et al. Complement is activated by IgG hexamers assembled at the cell surface. Science. 2014; 343:1260–1263. [PubMed: 24626930]
8. van Lookeren Campagne M, Wiesmann C, Brown EJ. Macrophage complement receptors and pathogen clearance. Cellular microbiology. 2007; 9:2095–2102. [PubMed: 17590164]
9. Muller-Eberhard HJ. The membrane attack complex of complement. Annual review of immunology. 1986; 4:503–528.
10. Bruhns P. Properties of mouse and human IgG receptors and their contribution to disease models. Blood. 2012; 119:5640–5649. [PubMed: 22535666]
11. Cullen SP, Martin SJ. Mechanisms of granule-dependent killing. Cell death and differentiation. 2008; 15:251–262. [PubMed: 17975553]
12. Freeman SA, Goyette J, Furuya W, Woods EC, Bertozzi CR, Bergmeier W, Hinz B, van der Merwe PA, Das R, Grinstein S. Integrins Form an Expanding Diffusional Barrier that Coordinates Phagocytosis. Cell. 2016; 164:128–140. [PubMed: 26771488]
13. Beron W, Alvarez-Dominguez C, Mayorga L, Stahl PD. Membrane trafficking along the phagocytic pathway. Trends in cell biology. 1995; 5:100–104. [PubMed: 14732163]
14. Clynes RA, Towers TL, Presta LG, Ravetch JV. Inhibitory Fc receptors modulate in vivo cytotoxicity against tumor targets. Nature medicine. 2000; 6:443–446.
15. Lopez-Albaitero A, Lee SC, Morgan S, Grandis JR, Gooding WE, Ferrone S, Ferris RL. Role of polymorphic Fc gamma receptor IIIa and EGFR expression level in cetuximab mediated, NK cell dependent in vitro cytotoxicity of head and neck squamous cell carcinoma cells. Cancer immunology, immunotherapy : CII. 2009; 58:1853–1864. [PubMed: 19319529]
16. Gul N, Babes L, Siegmund K, Korthouwer R, Bogels M, Braster R, Vidarsson G, ten Hagen TL, Kubes P, van Egmond M. Macrophages eliminate circulating tumor cells after monoclonal antibody therapy. The Journal of clinical investigation. 2014; 124:812–823. [PubMed: 24430180]
17. Tipton TR, Roghanian A, Oldham RJ, Carter MJ, Cox KL, Mockridge CI, French RR, Dahal LN, Duriez PJ, Hargreaves PG, Cragg MS, et al. Antigenic modulation limits the effector cell mechanisms employed by type I anti-CD20 monoclonal antibodies. Blood. 2015
18. Shim H. One target, different effects: a comparison of distinct therapeutic antibodies against the same targets. Experimental & molecular medicine. 2011; 43:539–549. [PubMed: 21811090]
19. Cragg MS, Morgan SM, Chan HT, Morgan BP, Filatov AV, Johnson PW, French RR, Glennie MJ. Complement-mediated lysis by anti-CD20 mAb correlates with segregation into lipid rafts. Blood. 2003; 101:1045–1052. [PubMed: 12393541]
20. Cragg MS, Glennie MJ. Antibody specificity controls in vivo effector mechanisms of anti-CD20 reagents. Blood. 2004; 103:2738–2743. [PubMed: 14551143]
21. Teeling J, Mackus W, Wiegman L, Van den Brakel J, Beers S, French R, van Meerten T, Ebeling S, Vink T, Slootstra J, Parren P, et al. The biological activity of human CD20 monoclonal antibodies is linked to unique epitopes on CD20. Journal of Immunology. 2006; 177:362–371.
22. Beers SA, Chan CH, James S, French RR, Attfield KE, Brennan CM, Ahuja A, Shlomchik MJ, Cragg MS, Glennie MJ. Type II (tositumomab) anti-CD20 monoclonal antibody out performs type I (rituximab-like) reagents in B-cell depletion regardless of complement activation. Blood. 2008; 112:4170–4177. [PubMed: 18583569]
23. Reichert, JM. Therapeutic monoclonal antibodies approved or in review in the European Union or the United States. The Antibody Society. 2017. Available at: http://www.antibodysociety.org/news/approved-antibodies/ Accessed: April 6, 2017

Europe PMC Funders Author Manuscripts

Europe PMC Funders Author Manuscripts

24. Golay J, Lazzari M, Facchinetti V, Bernasconi S, Borleri G, Barbui T, Rambaldi A, Introna M. CD20 levels determine the in vitro susceptibility to rituximab and complement of B-cell chronic lymphocytic leukemia: further regulation by CD55 and CD59. Blood. 2001; 98:3383–3389. [PubMed: 11719378]
25. Derer S, Bauer P, Lohse S, Scheel AH, Berger S, Kellner C, Peipp M, Valerius T. Impact of Epidermal Growth Factor Receptor (EGFR) Cell Surface Expression Levels on Effector Mechanisms of EGFR Antibodies. J Immunol. 2012
26. Bindon CI, Hale G, Waldmann H. Importance of antigen specificity for complement-mediated lysis by monoclonal antibodies. European journal of immunology. 1988; 18:1507–1514. [PubMed: 2973413]
27. Treumann A, Lifely M, Schneider P, Ferguson M. Primary structure of CD52. Journal of Biological Chemistry. 1995; 270:6088–6099. [PubMed: 7890742]
28. Cho HS, Mason K, Ramyar KX, Stanley AM, Gabelli SB, Denney DW Jr, Leahy DJ. Structure of the extracellular region of HER2 alone and in complex with the Herceptin Fab. Nature. 2003; 421:756–760. [PubMed: 12610629]
29. Haso W, Lee DW, Shah NN, Stetler-Stevenson M, Yuan CM, Pastan IH, Dimitrov DS, Morgan RA, Fitzgerald DJ, Barrett DM, Wayne AS, et al. Anti-CD22-chimeric antigen receptors targeting B-cell precursor acute lymphoblastic leukemia. Blood. 2013; 121:1165–1174. [PubMed: 23243285]
30. Varghese B, Widman A, Do J, Taidi B, Czerwinski DK, Timmerman J, Levy S, Levy R. Generation of CD8+ T cell-mediated immunity against idiotype-negative lymphoma escapees. Blood. 2009; 114:4477–4485. [PubMed: 19762487]
31. Kearney JF, Radbruch A, Liesegang B, Rajewsky K. A new mouse myeloma cell line that has lost immunoglobulin expression but permits the construction of antibody-secreting hybrid cell lines. J Immunol. 1979; 123:1548–1550. [PubMed: 113458]
32. Horton RM, Hunt HD, Ho SN, Pullen JK, Pease LR. Engineering hybrid genes without the use of restriction enzymes: gene splicing by overlap extension. Gene. 1989; 77:61–68. [PubMed: 2744488]
33. Sanchez AB, Nguyen T, Dema-Ala R, Kummel AC, Kipps TJ, Messmer BT. A general process for the development of peptide-based immunoassays for monoclonal antibodies. Cancer Chemother Pharmacol. 2010; 66:919–925. [PubMed: 20087593]
34. Perosa F, Favoino E, Caragnano MA, Dammacco F. Generation of biologically active linear and cyclic peptides has revealed a unique fine specificity of rituximab and its possible cross-reactivity with acid sphingomyelinase-like phosphodiesterase 3b precursor. Blood. 2006; 107:1070–1077. [PubMed: 16223774]
35. Won EY, Cha K, Byun JS, Kim DU, Shin S, Ahn B, Kim YH, Rice AJ, Walz T, Kwon BS, Cho HS. The structure of the trimer of human 4-1BB ligand is unique among members of the tumor necrosis factor superfamily. J Biol Chem. 2010; 285:9202–9210. [PubMed: 20032458]
36. Beum PV, Lindorfer MA, Taylor RP. Within peripheral blood mononuclear cells, antibody-dependent cellular cytotoxicity of rituximab-opsonized Daudi cells is promoted by NK cells and inhibited by monocytes due to shaving. J Immunol. 2008; 181:2916–2924. [PubMed: 18684983]
37. Xia MQ, Tone M, Packman L, Hale G, Waldmann H. Characterization of the CAMPATH-1 (CDw52) antigen: biochemical analysis and cDNA cloning reveal an unusually small peptide backbone. European journal of immunology. 1991; 21:1677–1684. [PubMed: 1711975]
38. Xia M, Hale G, Lifely M, Ferguson M, Campbell D, Packman L, Waldmann H. Structure of the CAMPATH-1 antigen, a glycosylphosphatidylinositol-anchored glycoprotein which is an exceptionally good target for complement lysis. Biochemical Journal. 1993; 293:633–640. [PubMed: 7688956]
39. Zent CS, Secreto CR, LaPlant BR, Bone ND, Call TG, Shanafelt TD, Jelinek DF, Tschumper RC, Kay NE. Direct and complement dependent cytotoxicity in CLL cells from patients with high-risk early-intermediate stage chronic lymphocytic leukemia (CLL) treated with alemtuzumab and rituximab. Leukemia research. 2008; 32:1849–1856. [PubMed: 18584865]
40. Dyer MJ, Hale G, Hayhoe FG, Waldmann H. Effects of CAMPATH-1 antibodies in vivo in patients with lymphoid malignancies: influence of antibody isotype. Blood. 1989; 73:1431–1439. [PubMed: 2713487]

Europe PMC Funders Author Manuscripts

41. Hu Y, Turner M, Shields J, Gale M, Hutto E, Roberts B, Siders W, Kaplan J. Investigation of the mechanism of action of alemtuzumab in a human CD52 transgenic mouse model. Immunology. 2009; 128:260–270. [PubMed: 19740383]
42. Uchida J, Hamaguchi Y, Oliver JA, Ravetch JV, Poe JC, Haas KM, Tedder TF. The innate mononuclear phagocyte network depletes B lymphocytes through Fc receptor-dependent mechanisms during anti-CD20 antibody immunotherapy. The Journal of experimental medicine. 2004; 199:1659–1669. [PubMed: 15210744]
43. James LC, Hale G, Waldmann H, Bloomer AC, Waldman H. 1.9 A structure of the therapeutic antibody CAMPATH-1H fab in complex with a synthetic peptide antigen. J Mol Biol. 1999; 289:293–301. [PubMed: 10366506]
44. Chen R, Knez JJ, Merrick WC, Medof ME. Comparative efficiencies of C-terminal signals of native glycophosphatidylinositol (GPI)-anchored proproteins in conferring GPI-anchoring. J Cell Biochem. 2001; 84:68–83. [PubMed: 11746517]
45. Bournazos S, Hart SP, Chamberlain LH, Glennie MJ, Dransfield I. Association of FcgammaRIIa (CD32a) with lipid rafts regulates ligand binding activity. J Immunol. 2009; 182:8026–8036. [PubMed: 19494328]
46. Bruhns P, Iannascoli B, England P, Mancardi DA, Fernandez N, Jorieux S, Daeron M. Specificity and affinity of human Fcgamma receptors and their polymorphic variants for human IgG subclasses. Blood. 2009; 113:3716–3725. [PubMed: 19018092]
47. Bruggemann M, Williams GT, Bindon CI, Clark MR, Walker MR, Jefferis R, Waldmann H, Neuberger MS. Comparison of the effector functions of human immunoglobulins using a matched set of chimeric antibodies. The Journal of experimental medicine. 1987; 166:1351–1361. [PubMed: 3500259]
48. Niederfellner G, Lammens A, Mundigl O, Georges GJ, Schaefer W, Schwaiger M, Franke A, Wiechmann K, Jenewein S, Slootstra JW, Timmerman P, et al. Epitope characterization and crystal structure of GA101 provide insights into the molecular basis for type I/II distinction of CD20 antibodies. Blood. 2011; 118:358–367. [PubMed: 21444918]
49. Banner DW, D'Arcy A, Janes W, Gentz R, Schoenfeld HJ, Broger C, Loetscher H, Lesslauer W. Crystal structure of the soluble human 55 kd TNF receptor-human TNF beta complex: implications for TNF receptor activation. Cell. 1993; 73:431–445. [PubMed: 8387891]
50. Shuford WW, Klussman K, Tritchler DD, Loo DT, Chalupny J, Siadak AW, Brown TJ, Emswiler J, Raecho H, Larsen CP, Pearson TC, et al. 4-1BB costimulatory signals preferentially induce CD8+ T cell proliferation and lead to the amplification in vivo of cytotoxic T cell responses. The Journal of experimental medicine. 1997; 186:47–55. [PubMed: 9206996]
51. Wyzgol A, Muller N, Fick A, Munkel S, Grigoleit GU, Pfizenmaier K, Wajant H. Trimer stabilization, oligomerization, and antibody-mediated cell surface immobilization improve the activity of soluble trimers of CD27L, CD40L, 41BBL, and glucocorticoid-induced TNF receptor ligand. J Immunol. 2009; 183:1851–1861. [PubMed: 19596991]
52. Nam KO, Kang H, Shin SM, Cho KH, Kwon B, Kwon BS, Kim SJ, Lee HW. Cross-linking of 4-1BB activates TCR-signaling pathways in CD8+ T lymphocytes. J Immunol. 2005; 174:1898–1905. [PubMed: 15699116]
53. Wallis R, Mitchell DA, Schmid R, Schwaeble WJ, Keeble AH. Paths reunited: Initiation of the classical and lectin pathways of complement activation. Immunobiology. 2010; 215:1–11. [PubMed: 19783065]
54. de Jong RN, Beurskens FJ, Verploegen S, Strumane K, van Kampen MD, Voorhorst M, Horstman W, Engelberts PJ, Oostindie SC, Wang G, Heck AJ, et al. A Novel Platform for the Potentiation of Therapeutic Antibodies Based on Antigen-Dependent Formation of IgG Hexamers at the Cell Surface. PLoS biology. 2016; 14:e1002344. [PubMed: 26736041]
55. Vidarsson G, Dekkers G, Rispens T. IgG subclasses and allotypes: from structure to effector functions. Frontiers in immunology. 2014; 5:520. [PubMed: 25368619]
56. Natsume A, In M, Takamura H, Nakagawa T, Shimizu Y, Kitajima K, Wakitani M, Ohta S, Satoh M, Shitara K, Niwa R. Engineered antibodies of IgG1/IgG3 mixed isotype with enhanced cytotoxic activities. Cancer research. 2008; 68:3863–3872. [PubMed: 18483271]

Europe PMC Funders Author Manuscripts

57. Davis SJ, van der Merwe PA. The kinetic-segregation model: TCR triggering and beyond. Nature immunology. 2006; 7:803–809. [PubMed: 16855606]
58. Choudhuri K, Wiseman D, Brown MH, Gould K, van der Merwe PA. T-cell receptor triggering is critically dependent on the dimensions of its peptide-MHC ligand. Nature. 2005; 436:578–582. [PubMed: 16049493]
59. Rudd PM, Morgan BP, Wormald MR, Harvey DJ, van den Berg CW, Davis SJ, Ferguson MA, Dwek RA. The glycosylation of the complement regulatory protein, human erythrocyte CD59. J Biol Chem. 1997; 272:7229–7244. [PubMed: 9054419]
60. Beers SA, French RR, Chan HT, Lim SH, Jarrett TC, Vidal RM, Wijayaweera SS, Dixon SV, Kim H, Cox KL, Kerr JP, et al. Antigenic modulation limits the efficacy of anti-CD20 antibodies: implications for antibody selection. Blood. 2010; 115:5191–5201. [PubMed: 20223920]
61. Ruffell B, Affara NI, Coussens LM. Differential macrophage programming in the tumor microenvironment. Trends in immunology. 2012; 33:119–126. [PubMed: 22277903]
62. Simpson TR, Li F, Montalvo-Ortiz W, Sepulveda MA, Bergerhoff K, Arce F, Roddie C, Henry JY, Yagita H, Wolchok JD, Peggs KS, et al. Fc-dependent depletion of tumor-infiltrating regulatory T cells co-defines the efficacy of anti-CTLA-4 therapy against melanoma. The Journal of experimental medicine. 2013; 210:1695–1710. [PubMed: 23897981]
63. Marson A, Kretschmer K, Frampton GM, Jacobsen ES, Polansky JK, MacIsaac KD, Levine SS, Fraenkel E, von Boehmer H, Young RA. Foxp3 occupancy and regulation of key target genes during T-cell stimulation. Nature. 2007; 445:931–935. [PubMed: 17237765]
64. McHugh RS, Whitters MJ, Piccirillo CA, Young DA, Shevach EM, Collins M, Byrne MC. CD4(+)CD25(+) immunoregulatory T cells: gene expression analysis reveals a functional role for the glucocorticoid-induced TNF receptor. Immunity. 2002; 16:311–323. [PubMed: 11869690]

Europe PMC Funders Author Manuscripts

Europe PMC Funders Author Manuscripts

Europe PMC Funders Author Manuscripts

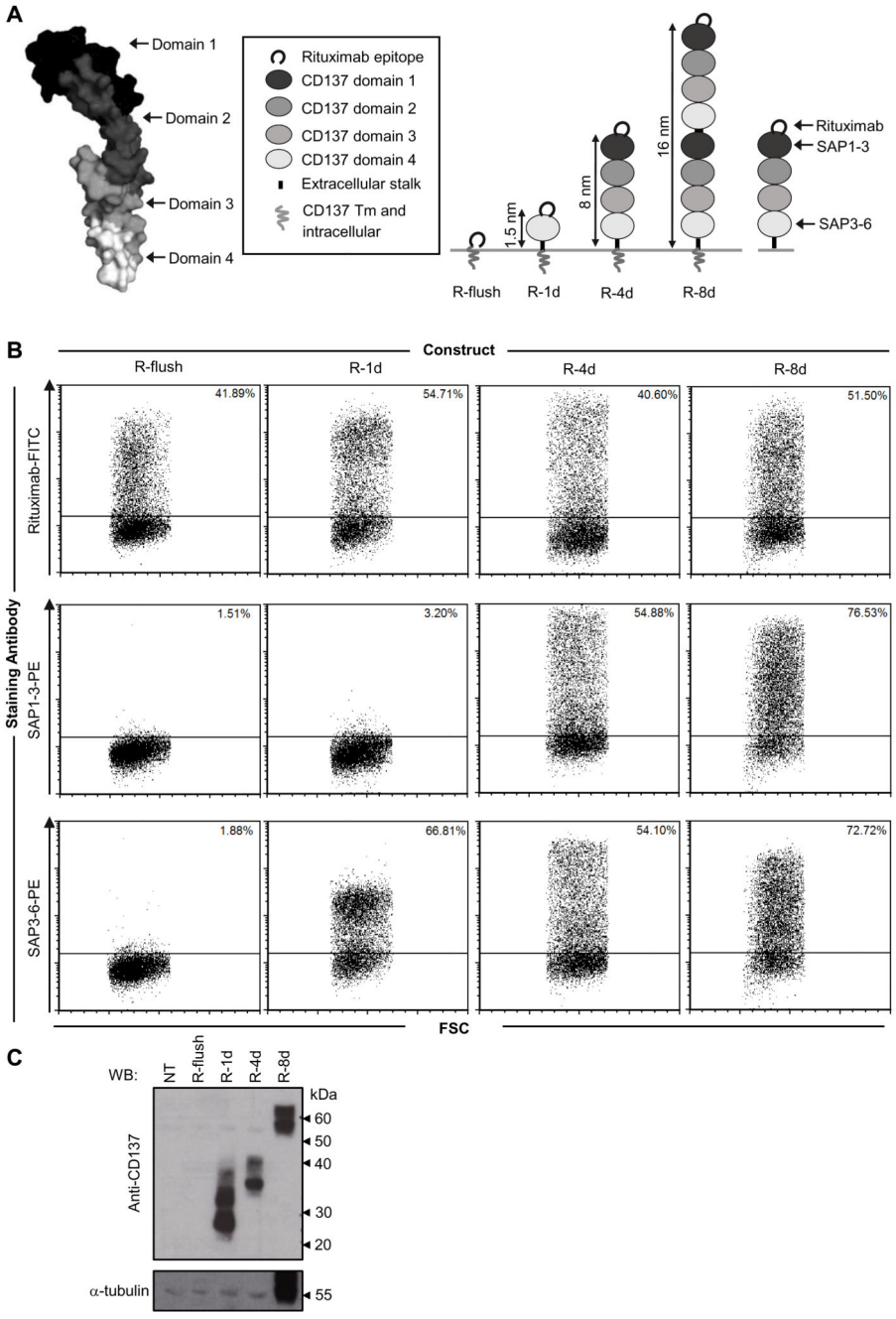

Figure 1. Generation and expression of fusion proteins displaying epitopes at different distances from the plasma membrane

A) Illustration representing the fusion proteins generated for use in the study. The resolved structure of TNFR1 was used as a model for the structure of CD137, and highlights its four clear cysteine-rich domains. Image generated in PyMol.1.3 using the uploaded PDB file: 1TNR. A peptide recognised by the anti-CD20 mAb rituximab (RTX) was attached to the N-terminal domain of human CD137 which contains 4 cysteine-rich domains (R-4d). Extracellular domains of CD137 were then either replicated, to generate an 8-domain construct (R-8d), or removed to produce a single domain protein (R-1d) as indicated. R-

flush consists of the RTX epitope attached to only the transmembrane (Tm) and intracellular domain of CD137. The domains bound by the anti-CD137 antibodies (SAP1-3 and SAP3-6) used to confirm expression are provided for reference. B) CHO-S cells were transfected with each of the constructs detailed and then cell surface expression assessed by flow cytometry using antibodies towards the RTX epitope and CD137 backbone 24 hours later. C) Confirmation of the size difference between R-4d and R-8d was achieved by western blot using polyclonal anti-CD137 antibody on whole cell lysates of the transfected CHO-S cells. α-tubulin was used as a loading control. NT = non-transfected CHO-S cell lysate.

Europe PMC Funders Author Manuscripts

Europe PMC Funders Author Manuscripts

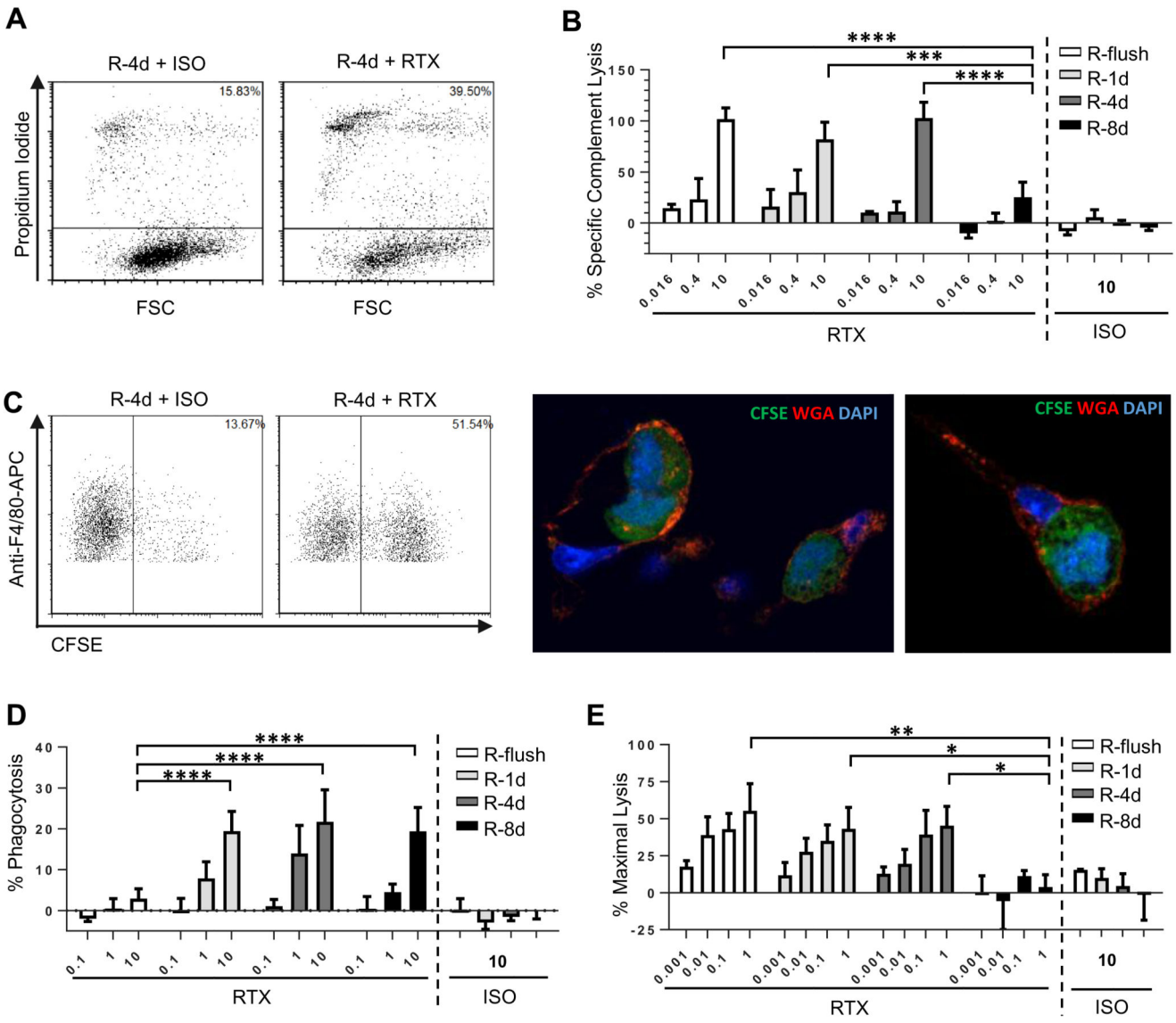

Figure 2. Comparison of cytotoxic activity engaged by rituximab when targeting CHO-S cells displaying the rituximab epitope at different distances from the plasma membrane

CHO-S cells transfected with each of the fusion proteins (Figure 1) were used as targets to investigate antibody effector mechanisms *in vitro*. A-B) Transfected CHO-S cells were labelled with RTX or an isotype control (ISO) and incubated with 15% human serum for 30 minutes. CDC was measured by flow cytometry using propidium iodide inclusion as a measure of cell lysis. A) shows representative data and B) results from n=3 independent experiments. C-D) CFSE labelled targets were opsonised with RTX or ISO before use as targets in an ADCP assay with murine BMDM. The percentage of BMDM which phagocytosed the target cells (defined as the $F4/80^{+}$ $CFSE^{+}$ population) was recorded and plotted above. C) shows representative flow cytometry data along with confocal imaging confirming phagocytosis of CFSE labelled targets. In the confocal imaging CFSE labelled targets are in green, wheat germ agglutinin (WGA) stained surface membranes are red and

Europe PMC Funders Author Manuscripts
Europe PMC Funders Author Manuscripts

DAPI-stained nuclei are blue. D) results from n=3 independent experiments. E) Calcein-AM labelled targets were opsonised with RTX or ISO before acting as targets in ADCC assays with human PBMC. For all experiments the mean and SD of three independent experiments are presented. Statistical significance was assessed using a two-way ANOVA test. * $p < 0.05$, ** $p < 0.005$, *** $p < 0.001$, **** $p < 0.0001$.

Europe PMC Funders Author Manuscripts

Europe PMC Funders Author Manuscripts

Europe PMC Funders Author Manuscripts

Europe PMC Funders Author Manuscripts

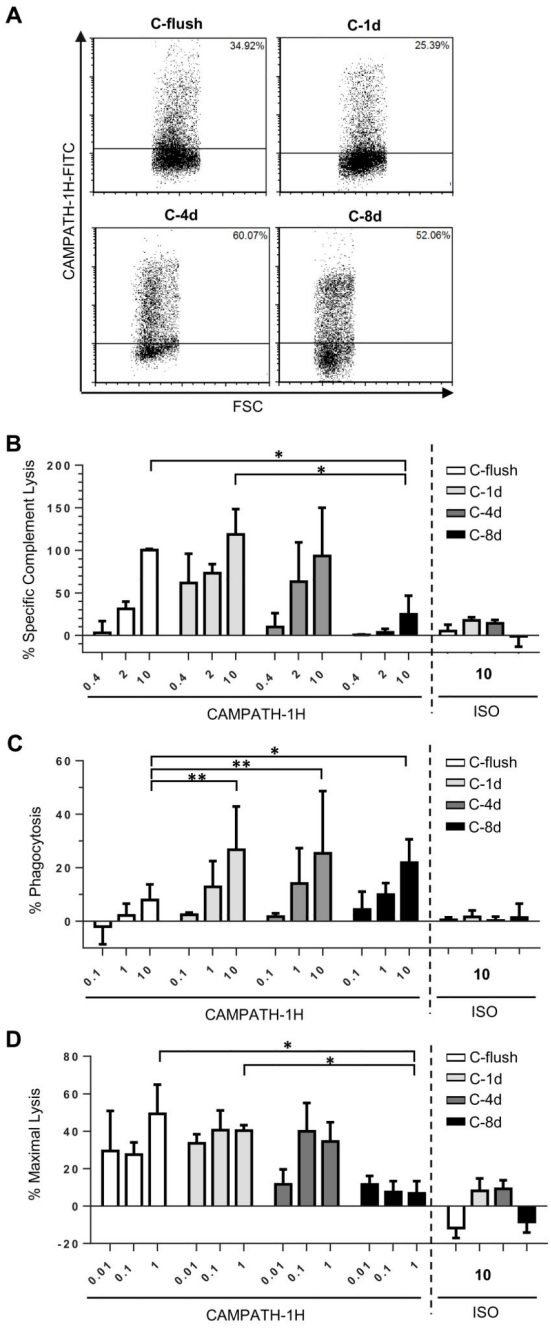

Figure 3. Comparison of cytotoxic activity engaged by CAMPATH-1H when targeting CHO-S cells displaying the CAMPATH epitope at different distances from the plasma membrane

A) CHO-S cells were transfected with each of the same CD137 backbone constructs as illustrated in Figure 1A but with the rituximab epitope replaced with an epitope recognised by CAMPATH-1H. 24 hours later cell surface expression was confirmed by flow cytometry using FITC-conjugated CAMPATH-1H. CHO-S cells expressing each of the fusion proteins were then used as targets in B) to assess sensitivity to CDC, C) for ADCP and D) for ADCC assay. The mean and SD of three independent experiments are presented. Statistical significance was assessed using a two-way ANOVA test. * $p < 0.05$, ** $p < 0.005$

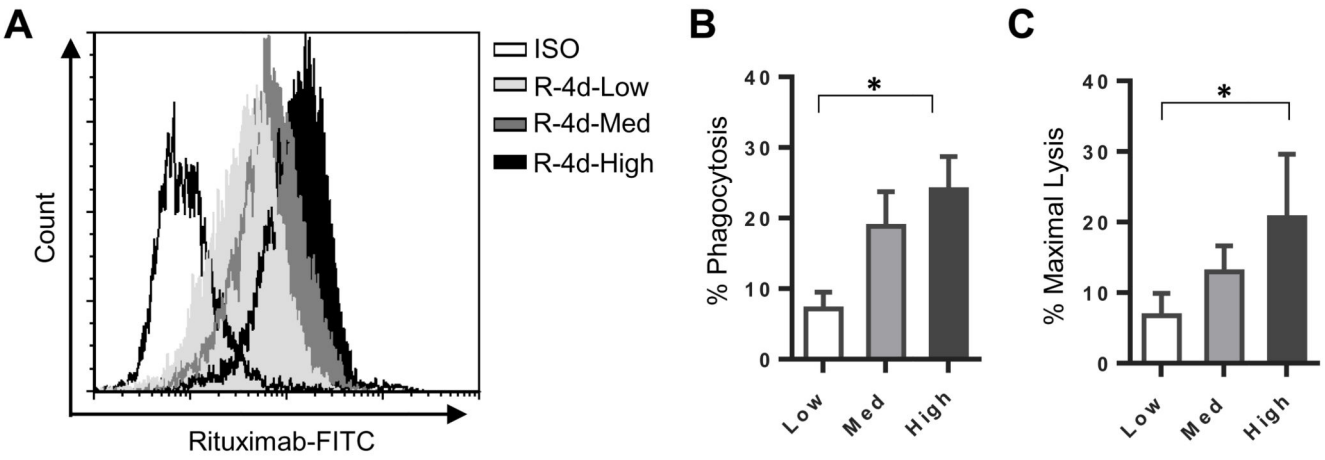

Figure 4. Importance of expression level for engagement of FcγR mediated mechanisms

A20 cells were transfected with the R-4d construct and stable clones expressing different levels at the cell surface were isolated. A) The clones were labelled with RTX-FITC or ISO-FITC and expression levels measured by flow cytometry. The three cell lines R-4d-Low, R-4d-Med and R-4d-High were used as targets in B) for ADCP and C) for ADCC. The mean and standard deviation of three independent experiments are presented. Statistical significance was assessed using a one-way ANOVA. * $p < 0.05$.

Europe PMC Funders Author Manuscripts

Europe PMC Funders Author Manuscripts

Europe PMC Funders Author Manuscripts

Europe PMC Funders Author Manuscripts

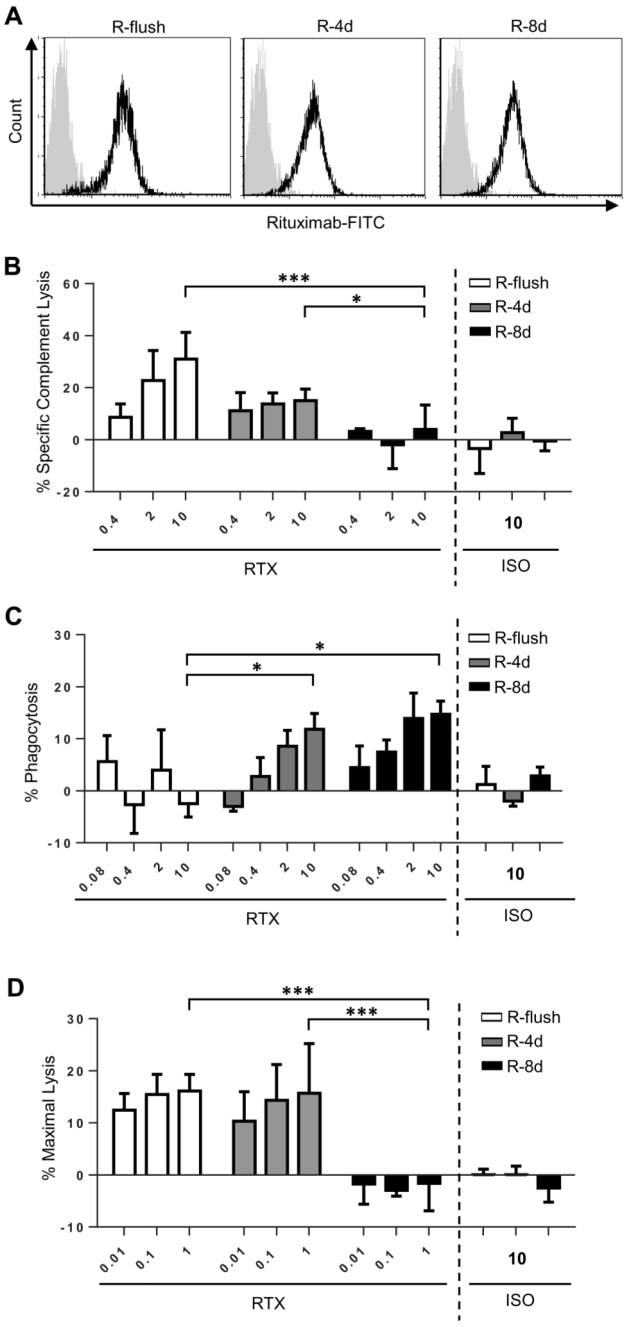

Figure 5. Comparison of cytotoxic activity engaged by rituximab when targeting A20 cells stably displaying the rituximab epitope at different distances from the plasma membrane

A) A20 cells were stably transfected to express the fusion proteins R-flush, R-4d and R-8d and then clones with equivalent levels of expression were selected. The flow cytometry data shows that the three cell lines express similar levels of the fusion protein when detected with FITC-conjugated rituximab. Grey overlay reflects staining with the ISO control. These cells were then used to assess B) CDC, C) ADCP and D) ADCC *in vitro*. The mean and standard deviation of three independent experiments are presented. Statistical significance was assessed using a two-way ANOVA test. * $p < 0.05$, *** $p < 0.001$.

Europe PMC Funders Author Manuscripts

Europe PMC Funders Author Manuscripts

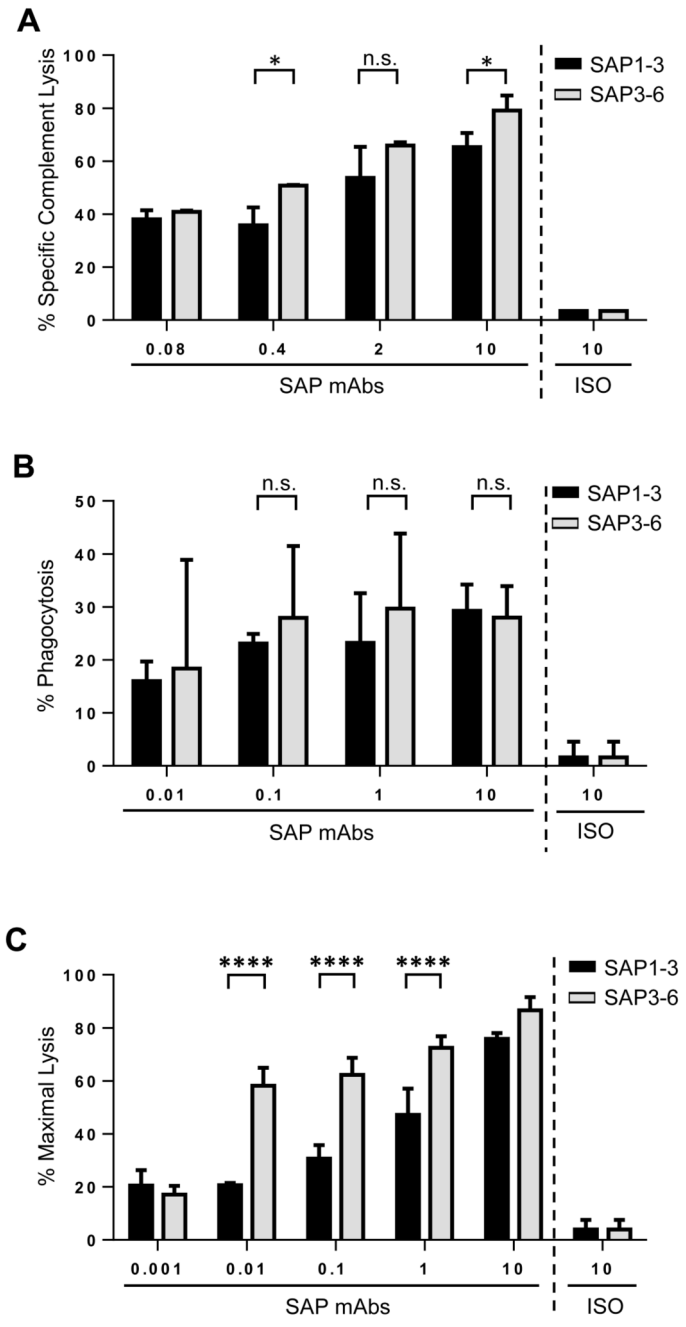

Figure 6. Comparison of cytotoxic activity engaged by mAb binding different domains of CD137

CHO-S cells expressing R-4d were labelled with different concentrations of SAP1-3 (binds membrane-distal domain of CD137) or SAP3-6 (binds membrane-proximal domain of CD137) and used as targets in A) CDC, B) ADCP and C) ADCC assays. For A) the mean and SD of three samples in a single experiment are plotted; B) the mean and SD of three independent experiments are plotted and C) is representative of three independent experiments. In all experiments statistical significance was assessed using a two-way ANOVA test. n.s. not significant, * $p < 0.05$, **** $p < 0.0001$.

Europe PMC Funders Author Manuscripts

Europe PMC Funders Author Manuscripts

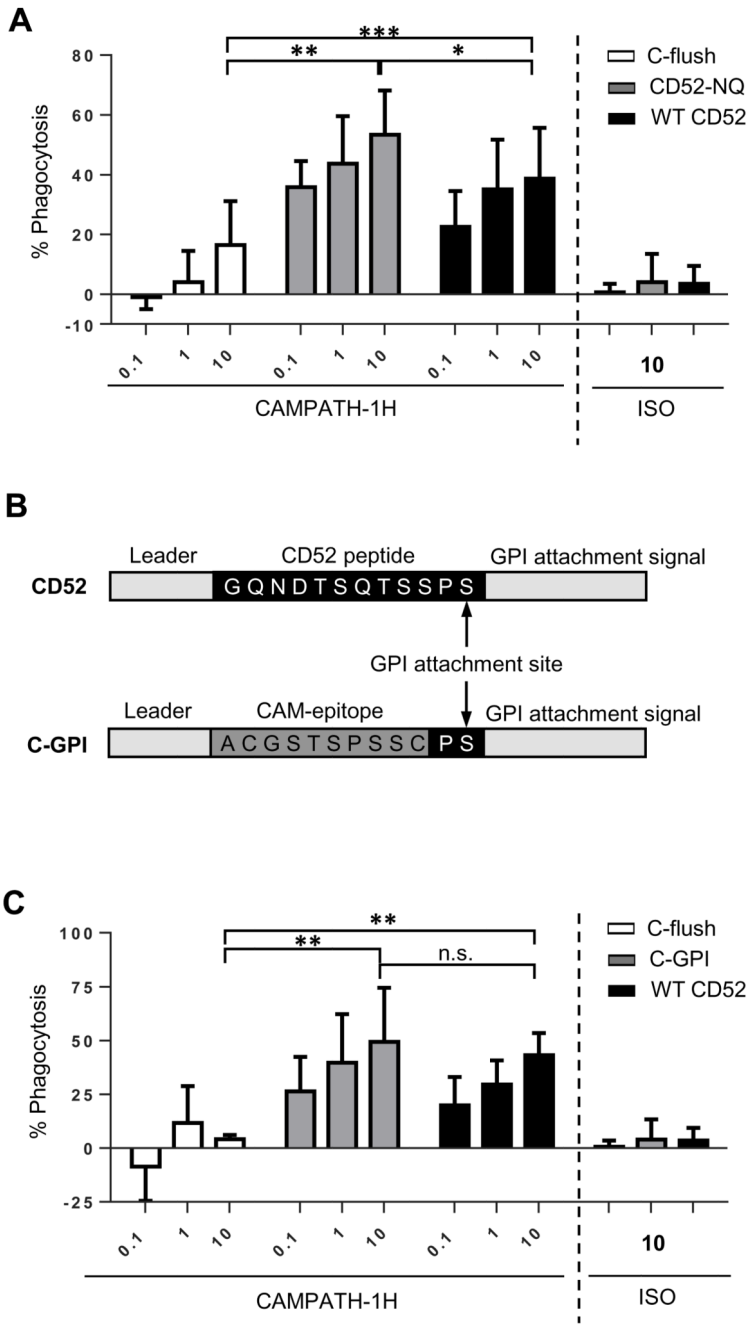

Figure 7. Importance of the GPI anchor of WT-CD52 for ADCP ability

A) A non-glyscoylated mutant of human CD52 (CD52-NQ) was generated and expressed in CHO-S cells. Its ability to facilitate ADCP of target cells when opsonised with CAMPATH-1H was then compared to CHO-S cells expressing C-flush or WT-CD52. B) Gene schematics for the generation of C-GPI consisting of the peptide CAMPATH-1H epitope attached to the same GPI anchor as CD52. C) The C-GPI construct was then generated and expressed in CHO-S cells. Its ability to facilitate ADCP of target cells when opsonised with CAMPATH-1H was compared to CHO-S cells expressing C-flush or WT-

CD52. The mean and SD of three independent experiments are presented. Statistical significance was assessed using a two-way ANOVA test. n.s. not significant, * $p < 0.05$, ** $p < 0.005$

Europe PMC Funders Author Manuscripts

Europe PMC Funders Author Manuscripts

Europe PMC Funders Author Manuscripts

Europe PMC Funders Author Manuscripts

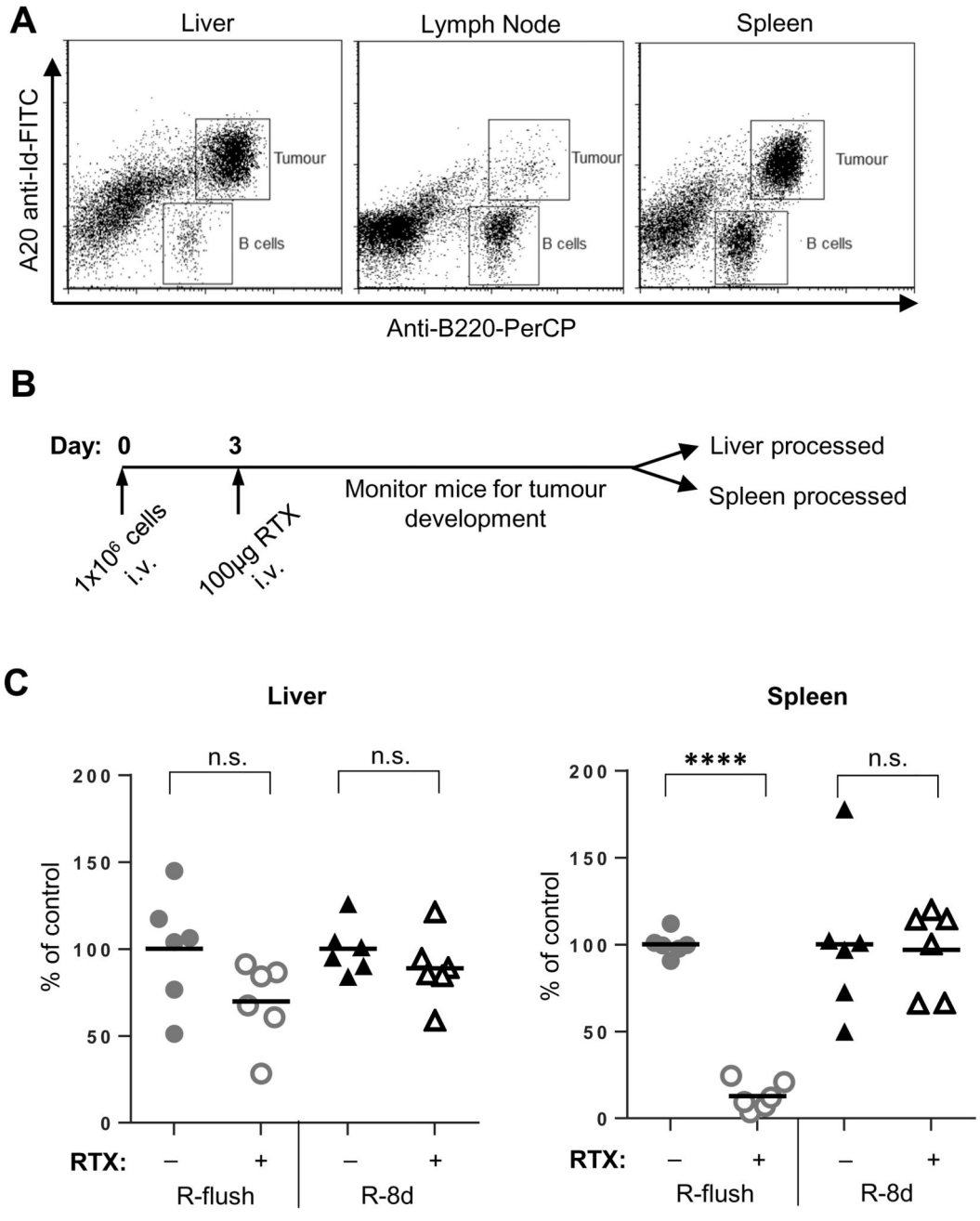

Figure 8. ***In vivo*** **clearance of A20 cells expressing different rituximab constructs following rituximab therapy**

A) WT female BALB/c mice were inoculated with $1x10^6$ A20 cells i.v. and screened for tumour development within the liver, spleen and lymph nodes in terminal animals by flow cytometry, as Idiotype+ B220+ cells. B) WT BALB/c mice were inoculated with A20 cells expressing either R-flush or R-8d on day 0, with 100µg Ritm2a or PBS given on day 3. C) Once mice had become terminal, the liver and spleen were harvested and the percentage of tumour cells identified by flow cytometry (Idiotype+ B220+). The percentage of tumour present for each individual mouse was normalised against the mean tumour burden within

the control group in each experiment. The data shows the results from six mice from two independent experiments. Statistical significance was assessed by a one-way ANOVA n.s. not significant, **** $p < 0.0001$.

Europe PMC Funders Author Manuscripts

Europe PMC Funders Author Manuscripts